Nonlinear Dynamics
Resonances, Chaos and Emittance growth in Circular Accelerators

Kazuhito Ohmi

KEK, Accelerator Lab

Joint US-CERN-Japan-Russia International Accelerator School 2019 Ion Colliders
JAS2019, Dubna, Russia

Oct. 28 - Nov. 7, 2019

Overview

Introduction

Emittance growth is one of important issues in accelerator physics. Incoherent emittance growth due to resonance and chaos is subject of nonlinear beam dynamics. We discuss nonlinear dynamics in circular accelerator,

1. Hamitonian and Lie formalism
2. Resonances and chaos
3. Applications to lepton and hadron colliders, and high intensity proton ring.

Hamiltonian in Accelerator/Beam Physics

Time variable is "s". 3rd dynamical variable $z = s - ct$, $z = s - vt$, $z = v(t_0 - t)$, or several choices. Any case 3rd variable is related to arrival time advance of partciles at "s".

$$H = \frac{E(\delta)}{P_0 v_0} - \left(1 + \frac{x}{\rho}\right)\sqrt{(1+\delta)^2 - p_x^2 - p_y^2} - \left(1 + \frac{x}{\rho}\right)\hat{A}_s \qquad (1)$$

Magnets and RF field are expressed by $\hat{A}_s = eA_s/P_0$.
Beam-beam force and space charge charge force are added as electric potential effectively.
In Circular accelerator, Hamiltonian is periodic for the circumference C.

$$H(x, p_x, y, p_y, z, \delta; s + C) = H(x, p_x, y, p_y, z, \delta; s) \qquad (2)$$

"s" dependent three degree of freedom

Symplectic transformation

Hamiltonian generates sympletic transformation.
Simplectic transformation of $\boldsymbol{x} = (x, p_x, y, p_y, z, \delta)$

$$\bar{\boldsymbol{x}} = \bar{\boldsymbol{x}}(\boldsymbol{x}) \tag{3}$$

satisfies

$$[\bar{x}_i, \bar{x}_j] \equiv \sum_{k,l=1}^{6} \frac{\partial \bar{x}_i}{\partial x_k} S_{kl} \frac{\partial \bar{x}_j}{\partial x_l} = S_{ij} \tag{4}$$

where $[,]$ is the Poisson bracket.

$$S = \begin{pmatrix} S_2 & 0 & 0 \\ 0 & S_2 & 0 \\ 0 & 0 & S_2 \end{pmatrix} \qquad S_2 = \begin{pmatrix} 0 & 1 \\ -1 & 0 \end{pmatrix}$$

When phase space is ellipse, the area of ellipse is kept a constant.
Emittance growth should be studied under keeping symplectic condition exactly.

Lie transform

Lie operator, Poisson bracket

$$: f : g = [f, g] = \sum_{i,j=1}^{6} \frac{\partial f}{\partial x_i} S_{ij} \frac{\partial g}{\partial x_j} = \sum_{a=1}^{3} \left(\frac{\partial f}{\partial x_a} \frac{\partial g}{\partial p_a} - \frac{\partial f}{\partial p_a} \frac{\partial g}{\partial x_a} \right) \tag{5}$$

Useful Formula

$$e^{:f:} g(x) = g(e^{:f:} x) \tag{6}$$

$$e^{:f:} e^{:g:} e^{-:f:} = exp(: e^{:f:} g :) \tag{7}$$

$exp(: A :)$ is symplectic, because $[e^{:A:} x, e^{:A:} p_x] = e^{:A:} [x, p_x] = 1....$

Equation of motion and its solution are represented by Lie operator,

$$\frac{d\boldsymbol{x}}{ds} = - : H : \boldsymbol{x} \qquad \bar{\boldsymbol{x}} = e^{-:H:s} \boldsymbol{x} \tag{8}$$

Examples for Lie operator

1. Quadrupole magnet with the length ℓ, $H = (p_x^2 + k_1 x^2)/2$,

$$\bar{x} = \cos(\sqrt{k_1}\ell) + \sin(\sqrt{k_1}\ell)/\sqrt{k_1}$$

$$\bar{p}_x = -\sqrt{k_1}\sin(\sqrt{k_1}\ell) + \cos(\sqrt{k_1}\ell)$$

2. Thin sextpole, $H = K_2 x^3/6$

$$e^{-H} p_x = p_x - \frac{K_2}{6}[x^3, p_x] + K_2^2[x^3, [x^3, p_x]] ... = p_x - \frac{K_2}{2}x^2 \qquad e^{-H} x = x$$

When Lie operator expansion is represenetd by finite series or is replaced by an analytic function, the map is symplectic.

Accelerator lattice ordered H_1, H_2...,

$$e^{-:H_1(\boldsymbol{x}):} e^{-:H_2(\boldsymbol{x}):} e^{-:H_3(\boldsymbol{x}):} e^{-:H_4(\boldsymbol{x}):} ... \tag{9}$$

This is opposite order against matrix form

$$\bar{\boldsymbol{x}} = ...M_4 M_3 M_2 M_1 \boldsymbol{x}$$

Generating function

Another way to integrate Hamiltonian with keeping symplecticity, when Lie operator expansion is infinite series.
For $H(x,p)$, use 2nd canonical transformation

$$F_2(x,\bar{p}) = x_a\bar{p}_a + H(x,\bar{p}) \tag{10}$$

$$p_a = \frac{\partial F_2}{\partial x_a} = \bar{p}_a + \frac{\partial H}{\partial x_a} \tag{11}$$

Implicit relation for $p = p(\bar{p})$ has to be solved as $\bar{p} = \bar{p}(p)$. It is possible.for only limited cases.

1. $H(x,p) = H_1(x) + H_2(p)$
2. H is linear for p.
3. Numerical solution for example, Newton-Raphson.
4. ....

More advanced examples

1. Crab waist scheme, $\exp(\mp : H_{cw} :)$ is operated before and after beam-beam collision.

$$H_{cw} = \frac{1}{4\theta_c} x^* p_y^{*2} \tag{12}$$

$$\bar{p}_x^* = p_x^* - [x^* p_x^{*2}/(4\theta_c, p_x^*] = p_x^* - p_y^{*2}/(4\theta_c)$$

$$\bar{y}^* = y^* - [x^* p_x^{*2}/(4\theta_c, y*] = y^* + x^* p_y^*/(2\theta_c)$$

2nd transformation shifts vertial waist proportional to x^*, $x^*/(2\theta_c)$.

2. Crab crossing, $\exp(\mp : H_{cc} :)$ is operated,

$$H_{cc} = \theta_c p_x^* z^* \tag{13}$$

$$\bar{x}^* = x - \theta_c [p_x^* z, x^*] = x^* + \theta_c z^*$$

$$\bar{\delta}^* = \delta^* - \theta_c [p_x^* z^*, \delta^*] = \delta^* - \theta_c p_x^*$$

First transformation gives a tilt θ_c in $x - z$ plane.

Examples (how to realize)

1. Crab waist scheme

$$H_{cw} = \frac{1}{4\theta_c} x^* p_y^{*2} \qquad (14)$$

$$T(s^* \to s) e^{-:H_{sext}(\boldsymbol{X}^*)} T(s \to s^*) = e^{-:H_{sext}(T(s^* \to s)\boldsymbol{X}^*):} = e^{-:H_{cw}(\boldsymbol{X}^*):}$$

$$1/(4\theta_c) = K_2 T_{11} T_{34}^2/2 \qquad T_{12} = T_{33} = 0$$

Choosing the phase difference $n\pi$ in horizontal and $\pi/2 + n'\pi$ for vertical from IP

2. Crab crossing with a half crossing angle θ_c.

$$H_{cc} = \theta_c p_x^* z^* \qquad (15)$$

Using crab cavity induces $H_{ccv} = V'xz$

$$\theta_c = V' T_{12} \qquad T_{11} = 0$$

The horizontal phase difference is chosen $\pi/2 + n\pi$

Collision with crossing angle

Crossing collision is transferred to head-on collision by

$$H_{cc} = \theta_c p_x^* z^* \tag{16}$$

where Lorentz contraction $(1/\cos\theta_c)$ in P_0 and z is neglected here. This transformation is compensated by crab cavities.

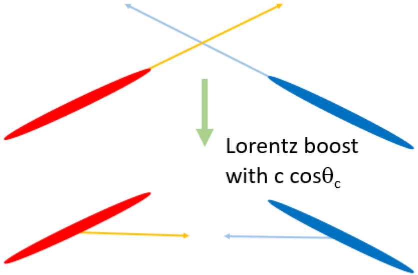

Figure: Schemetic view for crossing collision (K. Oide,PRA40,315(1989), K. Hirata, PRL74, 2228 (1995)).

One turn map

Transformation after one turn, one turn map, is expressed by

$$\begin{aligned} \mathcal{M} &= T_{0\rightarrow 1}e^{-:H_1:}T_{1\rightarrow 2}e^{-:H_2:}...e^{-:H_{N-1}:}T_{N-1\rightarrow N}e^{-:H_N:}T_{N\rightarrow 0} \\ &= T_0\prod_{i=1}^{N} exp(-:H_i(T_{0\rightarrow i}\boldsymbol{x}):) \end{aligned} \tag{17}$$

where T_0 is the revolution matrix at the position $s = 0 + (nC)$.

$$\mathcal{M} = T_0 e^{-:H:}$$

H can be trancated power series using or

$$H \approx \oint H(T_{0\rightarrow s}\boldsymbol{x}, s)ds$$

Linearized theory

$$H(s) = \frac{\delta^2}{2\gamma^2} - \frac{x\delta}{\rho(s)} + \frac{p_x^2 + p_y^2}{2} + \frac{x^2}{2\rho(s)^2} + \frac{K_1(s)}{2}(x^2 - y^2) - \frac{V'}{E_0} z^2 \tag{18}$$

For region with constant ρ and K_1, transfer matrix is obtained easily. 6×6 revolution matrix, which is symplectic.
Three eigenvalue with $e^{\pm i\mu_j}$ and conjugate pair of eigenvectors $(\boldsymbol{v}_j, \boldsymbol{v}_j^*)$ are obtained. Real and imaginary part of $\boldsymbol{v}_X$ gives X, P_X,

$$X = \frac{x}{\sqrt{\beta_x}} \quad P_X = \frac{\beta_x p_x + \alpha_x x}{\sqrt{\beta_x}} \qquad J_X = \frac{X^2 + P_X^2}{2} \quad \phi_x = -\tan^{-1}\frac{P_X}{X}$$

ϕ is betatron phase. $(J_X, \phi_x)$are canonical pair.
Y, Z are also expressed in the same way.
X, P_X rotate μ_x in the phase space after one revolution.

$$\begin{pmatrix} \bar{X} \\ \bar{P}_X \end{pmatrix} = \begin{pmatrix} \cos\mu_x & \sin\mu_x \\ -\sin\mu_x & \cos\mu_x \end{pmatrix} \begin{pmatrix} X \\ P_X \end{pmatrix}$$

Hamiltonian for one turn linear map is $H_0 = \mu_x J_x + \mu_y J_y - \mu_z J_z$

Nonlinear system

Hamiltonian generating one turn map.for Linear system with small nonlinear perturbation,

$$H(\boldsymbol{J},\phi) = H_0(\boldsymbol{J}) + U(\boldsymbol{J},\phi)$$

$\boldsymbol{\phi}$ is synchro-betatron phase at initial position s_0. Average over the synchro-betatron phase $\boldsymbol{\phi} = (\phi_x, \phi_y, \phi_z)$

$$\bar{U}(\boldsymbol{J}) = \frac{1}{2\pi}\oint U(\boldsymbol{J},\phi)d\boldsymbol{\phi}$$

Hamiltonian is epressed by averaged part which depends only on $\boldsymbol{J}$ and oscillation part,

$$H(J,\phi) = \bar{H}(J) + \hat{U}(J,\phi)$$

Tune

Synchro-betatron phase advance after one turn

$$\Delta\phi_j = \mu_i = \frac{\partial \bar{H}}{\partial J_i} \tag{19}$$

Tune $\nu_i = \mu_j/(2\pi)$ depends on the amplitude $\boldsymbol{J}$ in nonlinear system.

Source of nonlinear

1. Nonlinear magnets, sextupoles, octupoles....
2. Beam-beam force
3. Space charge force
4. Electron or ion cloud

How to calculate

1. Integrate nonlinear element in a ring.
2. Use computer pakkage, Taylar expansion, Differential Algebra...

Differential Algebra to evaluate nonlinear transformation of lattice magnets

Transformation of a magnet is represented by polynomial,

$$\boldsymbol{x}_1 = f_1(\boldsymbol{x}_0)$$

$$\boldsymbol{x}_2 = f_2(\boldsymbol{x}_1) = f_2(f_1(\boldsymbol{x}_0)) \equiv f_2 \circ f_1(\boldsymbol{x}_0)$$

$$....$$

$$.\boldsymbol{x}_n = f_n \circ ... \circ f_1(\boldsymbol{x}_0)..$$

Coefficient of the polynomial are calculated by computer. The polynomial is trancated by a certain order, for exmple 10, 15.... The transfer map expressed by the trancated polynomial is not symplectic.
We can have Lie operator expression for trancated polynomial,

$$\boldsymbol{x}_n = exp(- : H(\boldsymbol{x}_0) :)\boldsymbol{x}_0$$

Taking invariant part in $H = H(\boldsymbol{J})$, tune shift is evaluated.,

Nonlinearity of lattice magnets

Differential Algbra (SAD+) is executed for J-PARC MR.

$$
\begin{aligned}
H_{00} = & -4.5114 \times 10^{13} J_x^6 + 5.12293 \times 10^{16} J_x^5 J_y + 5.4158 \times 10^{12} J_x^5 \\
& -1.04751 \times 10^{16} J_x^4 J_y^2 + 5.1184 \times 10^{12} J_x^4 J_y + 1.01007 \times 10^9 J_x^4 \\
& -1.31809 \times 10^{16} J_x^3 J_y^3 + 6.64815 \times 10^{12} J_x^3 J_y^2 + 2.52657 \times 10^9 J_x^3 J_y \\
& +4.71257 \times 10^6 J_x^3 + 5.93598 \times 10^{15} J_x^2 J_y^4 - 2.2846 \times 10^{12} J_x^2 J_y^3 \\
& -2.07724 \times 10^8 J_x^2 J_y^2 - 5.02669 \times 10^6 J_x^2 J_y + 979.228 J_x^2 \\
& -2.37342 \times 10^{15} J_x J_y^5 - 5.60636 \times 10^{11} J_x J_y^4 - 1.00837 \times 10^9 J_x J_y^3 \\
& -3.71806 \times 10^6 J_x J_y^2 + 1578.47 J_x J_y + 5.75634 \times 10^{14} J_y^6 \\
& +3.76351 \times 10^{11} J_y^5 - 1.93481 \times 10^8 J_y^4 + 2.72899 \times 10^6 J_y^3 \\
& +722.764 J_y^2
\end{aligned}
$$

Resonance driving terms of H, which are function of ϕ, are also obtained.

Tune dependence

$$\nu(J) = \nu_0 + \frac{1}{2\pi}\frac{\partial H_{00}}{\partial J} \tag{20}$$

Tune shift is $\Delta\nu \sim 0.0005$ for J-PARC MR, where the aperture is 65 mm.mrad. The tune shift of space charge force is O(0.1).

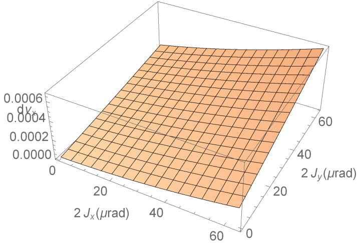

Figure: Amplitude dependent tune shift due to lattice nonlinear magnets in J-PARC MR.

Tune slope

$$2\pi \frac{d\nu(J)}{dJ} = \frac{\partial^2 H_{00}}{\partial J \partial J} \tag{21}$$

The second derivative, tune slope, is ~ 2000 for J-PARC MR. The value is compared with that of space charge force.

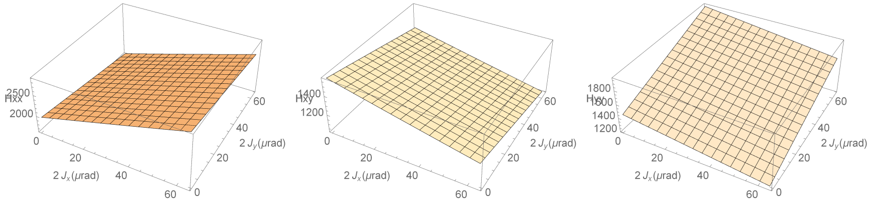

Figure: Tune slope due to lattice nonlinear magnets in J-PARC MR. (left) $\partial^2 H/\partial J_x^2$, (center) $\partial^2 H/\partial J_x \partial J_y$, (right) $\partial^2 H/\partial J_y^2$.

Potential induced by Transverse Gaussian charge distribution

Electric potential induced by Gaussian charge distribution,

$$\Phi(x,y,z) = \frac{e}{4\pi\epsilon_0}\int_0^\infty \frac{\exp\left(-\frac{x^2}{2\sigma_x^2+u}-\frac{y^2}{2\sigma_y^2+u}-\frac{z^2}{2\sigma_z^2+u}\right)-1}{\sqrt{(2\sigma_x^2+u)(2\sigma_y^2+u)(2\sigma_z^2+u)}}du \qquad (22)$$

A relativistic particle interacting with charge dirtribution with transverse Gaussian (unit charge)

$$U_G(x,y) = \frac{r_p}{\gamma}\int_0^\infty \frac{1-\exp\left(-\frac{x^2}{2\sigma_x^2+u}-\frac{y^2}{2\sigma_y^2+u}\right)}{\sqrt{(2\sigma_x^2+u)(2\sigma_y^2+u)}}du \qquad (23)$$

Beam-beam force

Collision with a half crossing angle θ_c.

$$U_{bb} = \frac{r_p}{\gamma} \int \lambda_p(z') U_G[x - \theta_c(z - z'), y] ds \tag{24}$$

Particles are in betatron oscillation even during small area of collision, $(s \sim s^*)$

$$x(s) = \sqrt{2\beta_x(s)J_x} \cos(\varphi_x(s) + \phi_x) \qquad y(s) = \sqrt{2\beta_y(s)J_y} \cos(\varphi_y(s) + \phi_y).$$

where $\varphi_{x,y}(s)$ is the betatron phase difference fom the interaction point s^*

$$\varphi_{x,y}(s) = \tan^{-1}\left(\frac{s}{\beta^*_{x,y}}\right). \tag{25}$$

$\phi_{x,y}$, which is the betatron phase at the interaction point, increases $2\pi\nu_{x,y}$ turn-by-turn. λ_p is line density of colliding beam at s. The density is function of the relative position from the beam center z'

$$\lambda_p(z') = \frac{N_p}{\sqrt{2\pi}} \exp\left(-\frac{z'^2}{2\sigma_z^2}\right) \tag{26}$$

where z' is related to s and z with $s = (z - z')/2$.

Fourier expansion of the beam-beam potential

$$U_{\boldsymbol{m}} = \frac{1}{(2\pi)^2}\int d\phi_x d\phi_y U_{bb} e^{i\boldsymbol{m}\boldsymbol{\phi}} \tag{27}$$

$$= \frac{1}{(2\pi)^2}\frac{r_p}{\gamma}\int \lambda_p ds \int d\boldsymbol{\phi} e^{i\boldsymbol{m}\boldsymbol{\phi}} \int_0^\infty \frac{1-\exp\left(-\frac{(x(s)-2s\sin\theta_c)^2}{2\sigma_x^2+u} - \frac{y(s)^2}{2\sigma_y^2+u}\right)}{\sqrt{2\sigma_x^2+u}\sqrt{2\sigma_y^2+u}} du$$

$$= \frac{r_p}{\gamma}\int ds \int_0^\infty \frac{\lambda_p(z')dt}{\sqrt{2+t}\sqrt{2r_{yx}+t}} \exp(-w_{x\theta}-w_y)$$

$$\sum_{l=-\infty}^{\infty}(-1)^{(m_x+l+m_y)/2} I_{(m_x-l)/2}(w_x) I_l(v_x) I_{m_y/2}(w_y) e^{-im_x\varphi_x - im_y\varphi_y}.$$

where $m_x - l$ and m_y are even numbers.

Tune spread in the amplitude space

$$\frac{\partial U_{00}}{\partial J_x} = \frac{1}{(2\pi)^2}\frac{Nr_p}{\gamma}\iint \lambda_p(z')dsd\phi\sqrt{\frac{\beta_x}{2J_x}}\cos(\varphi_x+\phi_x)F_x(x-2s\sin\theta_c,y)$$

$$\frac{\partial U_{00}}{\partial J_y} = \frac{1}{(2\pi)^2}\frac{Nr_p}{\gamma}\iint \lambda_p(z')dsd\phi\sqrt{\frac{\beta_y}{2J_y}}\cos(\varphi_y+\phi_y)F_y(x-2s\sin\theta_c,y) \quad (28)$$

F_x is wellknown formula represented by complex error function, w, [M. Bassetti, G. Erskine, CERN-ISR TH/80-06 (1980)]

$$F_y(x,y)+iF_x(x,y) = \frac{\sqrt{\pi}}{\Sigma}\left[w\left(\frac{x+iy}{\Sigma}\right)-\exp\left(-\frac{x^2}{2\sigma_x^2}-\frac{y^2}{2\sigma_y^2}\right)w\left(\frac{rx+iy/r}{\Sigma}\right)\right] \quad (29)$$

where $\Sigma=\sqrt{2(\sigma_x^2-\sigma_y^2)}$ and $r=\sigma_y/\sigma_x$.

Tune slope in the amplitude space

$$\frac{\partial^2 U_{00}}{\partial J_x^2} = \frac{1}{(2\pi)^2}\frac{Nr_p}{\gamma}\iint \lambda_p(z')dsd\phi \tag{30}$$

$$\left[-\frac{1}{2}\sqrt{\frac{\beta_x}{2J_x^3}}\cos(\varphi_x+\phi_x)F_x(x-2s\sin\theta_c,y)+\frac{\beta_x}{2J_x}\cos^2(\varphi_x+\phi_x)\frac{\partial F_x}{\partial x}\right]$$

$$\frac{\partial^2 U_{00}}{\partial J_y^2} = \frac{1}{(2\pi)^2}\frac{Nr_p}{\gamma}\iint \lambda_p(z')dsd\phi \tag{31}$$

$$\left[-\frac{1}{2}\sqrt{\frac{\beta_y}{2J_y^3}}\cos(\varphi_y+\phi_y)F_y(x-2s\sin\theta_c,y)+\frac{\beta_y}{2J_y}\cos^2(\varphi_y+\phi_y)\frac{\partial F_y}{\partial y}\right]$$

$$\frac{\partial^2 U_{00}}{\partial J_x\partial J_y} = \frac{1}{(2\pi)^2}\frac{Nr_p}{\gamma}\iint \lambda_p(z')dsd\phi\sqrt{\frac{\beta_x\beta_y}{4J_xJ_y}}\cos(\varphi_x+\phi_x)\cos(\varphi_y+\phi_y)\frac{\partial F_x}{\partial y} \tag{32}$$

Tune spead in KEKB, SuperKEKB and LHC

1. KEKB(left) : conventional type of e^+e^- collider based on flat beam collision.
2. SuprKEKB(center) : new type of e^+e^- collider based on large crossing (Piwinski) angle collision. $\Delta\nu_x \ll \Delta\nu_y$
3. LHC-head-on (right) : Hadron collider based on round beam collision.

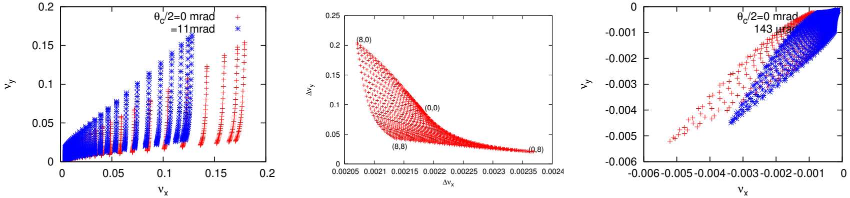

Figure: Tune spread due to the beam-beam interaction in KEKB, SuperKEKB and LHC.

Tune slope in SuperKEKB ($\beta_y = 3$ mm)

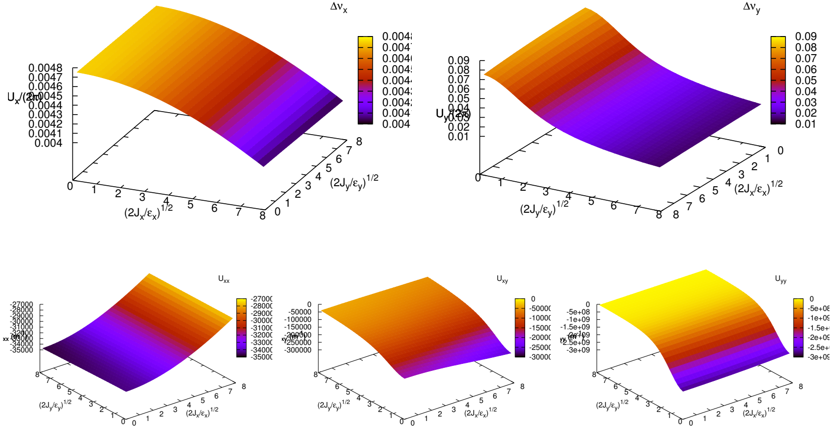

Figure: Tune spread and slope in SuperKEKB (detuned $\beta_y = 3$ mm).

Tune slope in SuperKEKB ($\beta_y = 0.3$ mm)

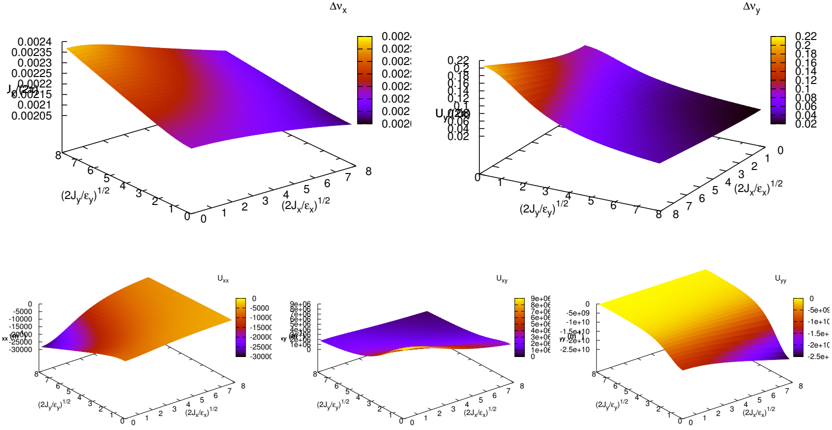

Figure: Tune spread and slope in SuperKEKB (design).

Space charge force

Assuming Gaussian distribution in the transverse phase space,

$$U(x,y,z)=\frac{N_p\lambda_p(z)r_p}{\beta^2\gamma^3}\int_0^\infty\frac{1-\exp\left(-\frac{x^2}{2\sigma_x^2+u}-\frac{y^2}{2\sigma_y^2+u}\right)}{\sqrt{2\sigma_x^2+u}\sqrt{2\sigma_y^2+u}}du \tag{33}$$

Dispersion should be taken into account

$$x(s)=\sqrt{2\beta_x(s)J_x}\cos(\varphi_x(s)+\phi_x)+\eta(s)\delta$$

$$U(\boldsymbol{J},\phi,z,s)=\oint_s ds' U(x,y,z;s') \tag{34}$$

$$=\frac{\lambda_p(z)r_p}{\beta^2\gamma^3}\oint_s ds'\int_0^\infty\frac{1-\exp\left(-\frac{x^2(s',s)}{2\sigma_x^2+u}-\frac{y^2(s',s)}{2\sigma_y^2+u}\right)}{\sqrt{2\sigma_x^2+u}\sqrt{2\sigma_x^2+u}}du$$

Tune spead in J-PARC MR

Space charge force for approximately round beam $\Delta\nu_x \sim \Delta\nu_y$. Tune spread is very large $\Delta\nu > 0.1$. The space charge force distribute in whole ring, while beam-beam force is localized at IP.

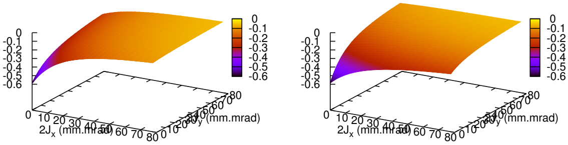

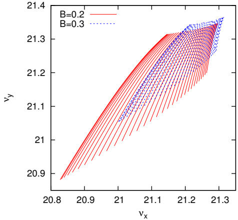

Tune slope

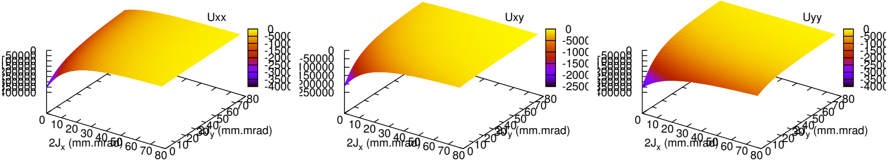

Figure: Tune slope due to space charge force in J-PARC MR.

Typical values are 10^5 near the beam position, and 10^4 outside of the beam area. Lattice magnets gave < 5000.
Space charge is dominant for the tune slope.

Resonance

Hamiltonian is expanded by Fourier series,

$$H = \mu J + U_{00}(\boldsymbol{J}) + \sum_{m_x, m_y \neq 0} U_{m_x,m_y}(\boldsymbol{J}) \exp(-im_x\phi_x - im_y\phi_y) \tag{35}$$

First and second terms in RHS characterize shift, spread and slope of tune.

$$\tilde{\mu}_i = \frac{\partial H}{\partial J_i} = \mu_i + \frac{\partial U_{00}}{\partial J_i} \tag{36}$$

Third term is averaged out for the tune shift due to the betatron phase variation. Resonance condition is expressed by ($\mu = 2\pi\nu$)

$$m_x\tilde{\nu}_x(\boldsymbol{J}) + m_y\tilde{\nu}_y(\boldsymbol{J}) = n. \tag{37}$$

where n is an integer. The resonance condition Eq.(38) gives a line in (J_x, J_y) space. $\boldsymbol{J}$ satisfying Eq.(38) is expressed by $\boldsymbol{J}_R$.

Resonance location

We calculte what amplitude a resonance occurs. Solve

$$m_x\tilde{\mu}_x(\boldsymbol{J}) + m_y\tilde{\mu}_y(\boldsymbol{J}) = 2\pi n. \qquad (38)$$

for several resonances for a pp collider as an example.

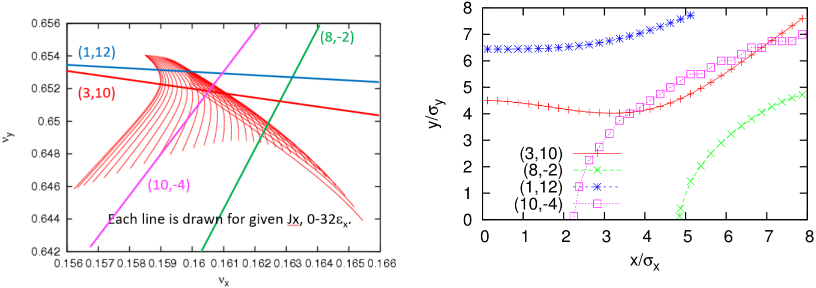

Figure: Tune spread area and resonance in the amplitude space for a hadron collider, SPPC (x-crossing), long range collisions are included.

Behavior near resonance

Hamiltonian is expanded near $\boldsymbol{J}_R$ as

$$U_{00}(\boldsymbol{J}) = U_{00}(\boldsymbol{J}_R) + \left.\frac{\partial U_{00}}{\partial \boldsymbol{J}}\right|_{\boldsymbol{J}_R} (\boldsymbol{J} - \boldsymbol{J}_R)$$
$$+ (\boldsymbol{J} - \boldsymbol{J}_R)^t \frac{1}{2} \left.\frac{\partial^2 U_{00}}{\partial \boldsymbol{J} \partial \boldsymbol{J}}\right|_{\boldsymbol{J}_R} (\boldsymbol{J} - \boldsymbol{J}_R) \tag{39}$$

Third term in RHS is characterized by the tune slope

$$2\pi \frac{\partial \nu_i}{\partial J_j} = 2\pi \frac{\partial \nu_j}{\partial J_i} = \frac{\partial^2 U_{00}}{\partial J_i \partial J_j} \tag{40}$$

Behavior near resonance

Canonical transformation for new variable $\boldsymbol{P}$ and ψ is considered

$$F_2(\boldsymbol{P},\phi) = (J_{x,R} + m_x P_1 + m_{x,2} P_2)\phi_x + (J_{y,R} + m_y P_1 + m_{y,2} P_2)\phi_y$$

Choosing $m_{x,2} = 0, m_{y,2} = 1$ independent of (m_x, m_y).

$$P_1 = \frac{J_x - J_{x,R}}{m_x} \qquad \psi_1 = m_x\phi_x + m_y\phi_y \tag{41}$$

$$P_2 = (J_y - J_{y,R}) - \frac{m_y}{m_x}(J_x - J_{x,R}) \qquad \psi_2 = \phi_y$$

Hamiltonian for $\boldsymbol{J}$ dependent terms is now given by

$$H_{00} = U_{00} \approx \frac{\Lambda}{2} P_1^2, \tag{42}$$

where

$$\Lambda \equiv m_x^2 \frac{\partial^2 U_{00}}{\partial J_x^2} + m_x m_y \frac{\partial^2 U_{00}}{\partial J_x \partial J_y} + m_y^2 \frac{\partial^2 U_{00}}{\partial J_y^2}. \tag{43}$$

Resonance width

The resonance term, which is third term of RHS in Eq.(35), drives resonances. The resonance strengths $U_{\boldsymbol{m}}$ as function of $\boldsymbol{J}$ are approximated to be those at $\boldsymbol{J}_R$

$$U_{\boldsymbol{m}}(\boldsymbol{J}) \approx U_{\boldsymbol{m}}(\boldsymbol{J}_R) \qquad \boldsymbol{m} = (m_x, m_y). \tag{44}$$

Hamiltonian for the standard model is given as

$$H = \frac{\Lambda}{2} P_1^2 + U_{\boldsymbol{m}}(\boldsymbol{J}_R) \cos \psi_1. \tag{45}$$

Phase space structure near resonances are characterized by the resonance width. The resonance width is given by

$$\Delta P_1 = 4\sqrt{\frac{U_{\boldsymbol{m}}}{\Lambda}} \qquad \Delta J_x = 4 m_x \sqrt{\frac{U_{\boldsymbol{m}}}{\Lambda}}. \tag{46}$$

Schemetic view of Resonance

Particle oscillates harmonic motion in the vicinity of the resonance point. Detuning from the resonance condition, separatrix is seen.

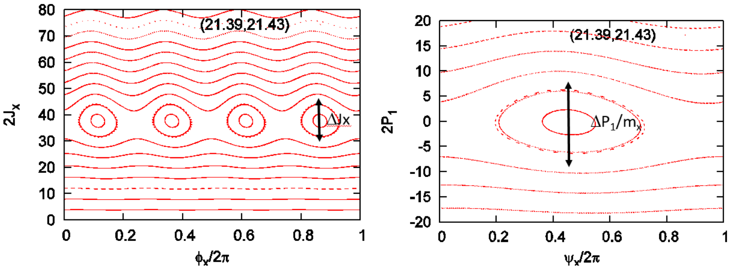

Figure: Resonance with base of (J_x, ϕ_x) and (P_1, ψ_1).

Resonances causes emittance growth, but week growth.
Coupling to synchrotron motion is important as shown later.

Calulation of resonance width

Resonance driving term, tune slope and resonance width depend on the amplitude in which the resonance condition is satisfied. The stochasititisy parameter is lower than 1. Weak chaos.

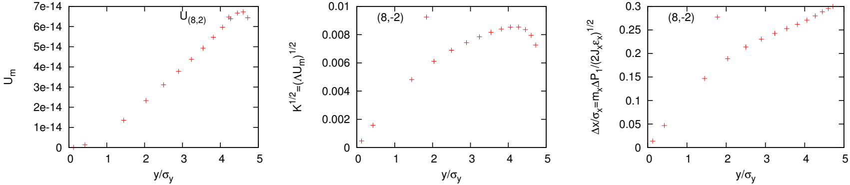

Figure: Resonance driving term, stochasticity parameter and resonance width.

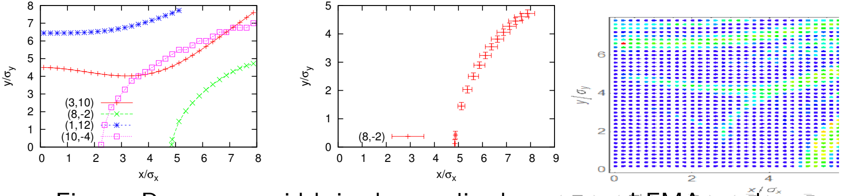

Figure: Resonance width in the amplitude space and FMA result.

Resonance with finte z

For finite z, tune spread area decreases.

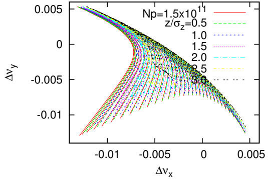

Figure: Tune spread for finte synchrotron amplitudes.

Beam-beam and Space charge forces are symmetric for x and y. Only even resonances are induced. Odd resonances are induced for finite z.

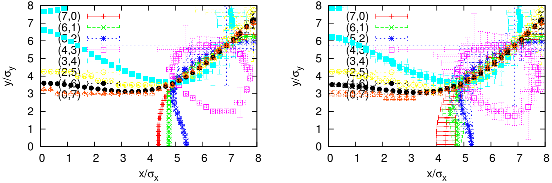

Figure: Resonance width in the transverse amplitude space for zero and finite synchrotron amplitude.

Synchrotron motion

Synchrotron motion is very sow compre with betatron motion.

$$z = \sqrt{2\beta_z J_z}\cos\phi_z \qquad \delta = \sqrt{2J_z/\beta_z}\sin\phi_z. \tag{47}$$

$\phi_z = \mu_z t$ increase as turn number t.
Resonance driving term, tune slope are modulated by the synchrotron motion. Fourier component for te synchrotron tune is calculated as

$$U_{bb} = U_{\boldsymbol{o},0} + \sum_{m_z \neq 0} U_{\boldsymbol{o},m_z} e^{-im_z\phi_z} + \sum_{\boldsymbol{m}\neq 0, m_z} U_{\boldsymbol{m},m_z} e^{-i\boldsymbol{m}\cdot\boldsymbol{\phi} - im_z\phi_z} \tag{48}$$

$$U_{\boldsymbol{m},m_z}(\boldsymbol{J}, J_z) = \frac{1}{2\pi}\int U_{\boldsymbol{m}}(\boldsymbol{J}, z)e^{im_z\phi_z}d\phi_z \tag{49}$$

The synchrotron tune is slow and can be comparable with the motion near the resonance. $U_{\boldsymbol{o},m_z}$ term should be considered regardless of the resonance condition.

Synchrotron side band

The resonance condition of $\boldsymbol{J}$ for a particle with J_z is

$$m_x\nu_x(\boldsymbol{J},J_z)+m_y\nu_y(\boldsymbol{J},J_z)+m_z\nu_z=n \tag{50}$$

$$\bar{U}(\boldsymbol{J},J_z)=U_{\boldsymbol{0},0}(\boldsymbol{J},J_z)+\sum_{\boldsymbol{m}\neq 0}U_{\boldsymbol{m},m_z}(\boldsymbol{J},J_z)e^{-i\boldsymbol{m}\cdot\boldsymbol{\phi}-im_z\phi_z} \tag{51}$$

Focusing the resonance, Hamiltonian is expressed by

$$\bar{H}=\bar{U}=\frac{\Lambda_{\boldsymbol{m}}}{2}P_1^2+U_{\boldsymbol{m},0}(\boldsymbol{J}_R,J_z)\cos\psi_1 \tag{52}$$

$$\Lambda_{\boldsymbol{m}}\equiv m_x^2\frac{\partial^2 U_{\boldsymbol{0},0}}{\partial J_x^2}+2m_xm_y\frac{\partial^2 U_{\boldsymbol{0},0}}{\partial J_x\partial J_y}+m_y^2\frac{\partial^2 U_{\boldsymbol{0},0}}{\partial J_y^2}. \tag{53}$$

$\Delta\nu_z=\partial U/\partial J_z$ is neglected. Synchrotron oscillation is treated as external oscillation.

Modulation due to synchrotron motion

Synchrotron frequency component,

$$U_{\boldsymbol{O}} \equiv U_{\boldsymbol{O},0} + \sum_{m_z \neq 0} U_{\boldsymbol{O},m_z} e^{-im_z\phi_z} \tag{54}$$

The potential is expand around $\boldsymbol{J}_R$ as follows,

$$\begin{aligned} U_{\boldsymbol{O}}(\boldsymbol{J}, J_z, t) &= U_{\boldsymbol{O}}(\boldsymbol{J}_R) + \left.\frac{\partial U_{\boldsymbol{O}}}{\partial \boldsymbol{J}}\right|_{\boldsymbol{J}_R} \cdot (\boldsymbol{J} - \boldsymbol{J}_R) \\ &= \sum_{m_z \neq 0} \frac{\partial U_{\boldsymbol{O},m_z}}{\partial \boldsymbol{J}} \cdot (\boldsymbol{J} - \boldsymbol{J}_R) e^{-im_z\mu_z t} = \sum_{m_z \neq 0} \frac{\partial U_{\boldsymbol{O},m_z}}{\partial \boldsymbol{J}} \cdot \boldsymbol{m} P_1 e^{-im_z\mu_z t} \end{aligned} \tag{55}$$

where U and its derivatives are evaluated at $\boldsymbol{J}_R$. Linear term for P_2, which gives an oscillation of P_2, is neglected.

Resonance overlap between synchrotron side bands

The standardized transfer map for $H = \bar{H} + \hat{U}$ is given by

$$
\begin{aligned}
I_{t+1} &= I_t + \sum_{m_z} K_{m_z} \sin\theta_t \cos(m_z \mu_z t) \qquad (56)\\
\theta_{t+1} &= \theta_t + I_{t+1} + \sum_{m_z \neq 0} \frac{\partial U_{\boldsymbol{o},m_z}}{\partial \boldsymbol{J}} \cdot \boldsymbol{m} \cos(m_z \mu_z t).
\end{aligned}
$$

where $I = \Lambda_{\boldsymbol{m}} P_1$, $\theta = \psi_1$ and $K_{m_z} = \Lambda_{\boldsymbol{m}} U_{\boldsymbol{m},m_z}$.

Resonance overlaps conditions

1. The resonance width of each sideband (with even m_z) is larger than the resonance spacing μ_z between sidebands,

$$3\sqrt{K_{m_z}} = 3\sqrt{\Lambda_{\boldsymbol{m}} U_{\boldsymbol{m},m_z}} > 2\mu_z \qquad (57)$$

2. Chaotic area due to the mudulation is larger than the resonance width or separation

$$\Delta P_1 = \mathrm{Max}_{m_z} \left(\frac{1}{\Lambda} \frac{\partial U_{\boldsymbol{o},m_z}}{\partial \boldsymbol{J}} \cdot \boldsymbol{m} \right) \qquad (58)$$

Example of overlap between synchrotron side bands

SPPC (China) is hadron collider which is competitor of FCC-hh.

1. 7-th order resonance
2. Resonances m_z=0 and 2 canoverlap.
3. STochstic area due to modulation is narrower thanthe resonance width, but contributes the overlap.

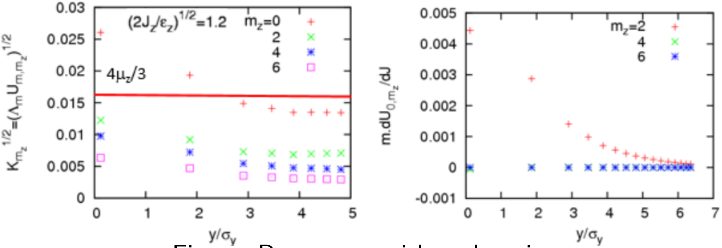

Figure: Resonance with crab waist.

Resonance overlap enhances emittance growth remarkably.

Resonance suppression in Crab Waist

Crab waist scheme

$$H_{cw} = \frac{1}{4\theta_c} x^* p_y^{*2} \tag{59}$$

$$T_{rev} e^{-:H_{cw}(\boldsymbol{x}^*):} e^{-:U_{bb}(\boldsymbol{x}^*):} e^{:H_{cw}(\boldsymbol{x}^*):} = T_{rev} e^{-:U_{bb}(e^{-:H_{cw}(\boldsymbol{x}^*):}\boldsymbol{x}^*)} \tag{60}$$

Particles with x

$$U_{bb} = \int \lambda(z') U_G(x + \theta_c(z - z'), y + p_y s; s) ds \qquad s = (z - z')/2. \tag{61}$$

Large contribution $x \approx -2\theta_c s$.

$$U_{bb} \approx \int \lambda(z') U_G(x + 2\theta_c s, y - x p_y/(2\theta_c); s) ds \tag{62}$$

The second argument $y + xp_y/(2\theta_c)$ induces resonances on $x - y$ coupling. The resonances are compensated by the crab waist transformation, $y \to y + xp_y/(2\theta_c)$

Resonance width for $\nu_x + 4\nu_y = 3$ w/wo crab waist

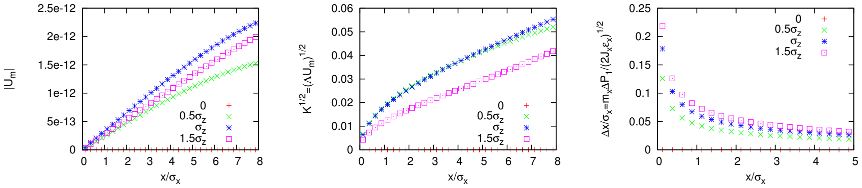

Figure: Resonance without crab waist.

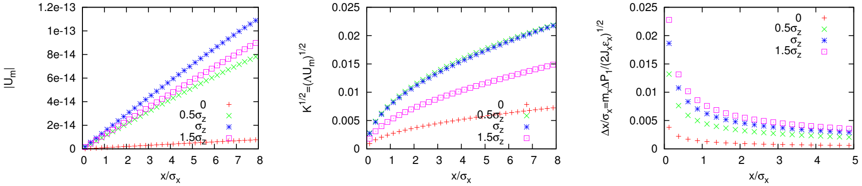

Figure: Resonance with crab waist.

The resonance width with crab waist is one order lower than that without crab waist.

Super-periodicity and structure resonance

J-PARC MR ring has superperiodicity of three. It is sufficient to consider 1/3 ring, $m_x\nu_x/3 + m_y\nu_y/3 = n$. Namely, only structure resonances $m_x\nu_x + m_y\nu_y = 3n$ exist under the perfect superperidicity. Nonstructure resonances , $m_x\nu_x + m_y\nu_y = n'(\neq 3n)$ do not exist.

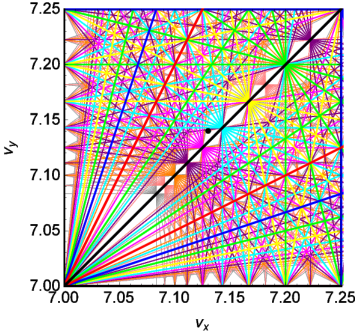

Figure: .Tune diagram near $(\nu_x/3, \nu_y/3) = (7.13, 7.143)$, where total tune is (21.35,21.4).

Breaking of Superperiodicity and nonstructure resonance

In real accelerator, superperiodicity is broken by various errors.
Non-structure resonances appear.

$$\mathcal{M} = \exp\left(-H_{00}^{(3)} - H_{\boldsymbol{m}}^{(3)}\right)\exp\left(-H_{00}^{(2)} - H_{\boldsymbol{m}}^{(2)}\right)\exp\left(-H_{00}^{(1)} - H_{\boldsymbol{m}}^{(1)}\right) \quad (63)$$

$$H_{00}^{(2,3)} + H_{\boldsymbol{m}}^{(2,3)} = H_{00}^{(1)} + H_{\boldsymbol{m}}^{(1)} + \Delta H_{00}^{(2,3)} + \Delta H_{\boldsymbol{m}}^{(2,3)} \quad (64)$$

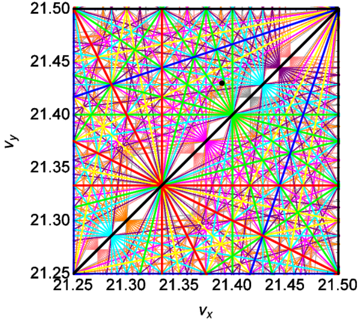

Figure: .Tune diagram near $(\nu_x, \nu_y) = (21.39, 21.43)$

How to evaluate nonstructure resonances

Error sources can

1. Deviations of beta function, phase and other Twiss parameters at nonlinear elements.
2. Deviations of strength of nonlinear elements is more reliable than Twiss.

Nonstructure resonances can be evaluated by measured Twiss parameters. Integrate space charge potential using the measured Twiss parameters. [K.Ohmi, HB2014, ICAP15, IPAC16,17]

Summary

1. Hamiltonian formalism and Lie operator approach have been used to study nonlinear dynamics in accelerators.
2. Most of works to study emitance growth has relied numerical simulations.
3. Theory for resonances and chaos is important to understand physics of the emittance growth.
4. Stocasticity parameter of accelerators is not large ($K \sim 0.01$) as chaotic system.
5. Resonance overlap between synchrotron side bands andmudulationdue to synchrotron oscillation enhance emittance growth.
6. Theory is also helpful to understand new technique using crab cavity and crab waist.
7. Breaking of Superperiodicity and nonstructure resonance may be interesting in the future.

References

H. Goldstein, Classical Mechanics
Addison-Wesley Publishing Company, Inc.

A.J. Dragt, Lecture on Nonlinear Orbit Dynamics
AIP Conf. Proc. 87, 147 – 313 (1982).

B.V. Chirikov, A Universal Instability of Many-Dimensional Oscillator System
Physics Report 52, 263-379 (1979).

J. L. Tennyson, The dynamics of the beam-beam interaction
AIP Conf. Proc. 87, 345 – 394 (1982).

A.J. Lichtenberg, M.A. Lieberman, Regular and Chaotic Dynamics
Applied Mathematical Sciences Vol. 38, 1992 Springer-Verlag New York, Inc.

The End
Thank you for your attention